EXTENDED EXPERIMENTAL PROCEDURES

FRET analysis

FRET was detected between DSCR1 and phospho-FMRP using acceptor photo-bleaching methods. The DIV 21 cultured hippocampal neurons were stained against phospho-FMRP and DSCR1 primary antibodies or PSD95 and DSCR1 primary antibodies, respectively, and then detected with secondary antibodies labeled with Alexa 488 and Alexa 555, which can be one pair of donor and acceptor in the FRET analysis. We analyzed fluorescence and FRET using Leica SP5 confocal microscope with FRET analysis software. The red fluorescence (555 nm) of acceptor was bleached for 5 seconds using a 561 nm laser in the dendritic spine regions, then the intensity of donor green fluorescence (488 nm) was detected before and after photo-bleaching of the acceptor. The FRET efficiency was determined using the FRET acceptor bleaching wizard software in the Leica confocal. For live cell acceptor bleaching, HEK293 cells were co-transfected using standard Lipofectamine^{TM} method. Briefly, ~200 ng of plasmid DNA was used per construct per $2.0x10^3$ HEK cells per glass covered bottom dish (In Vitro Scientific). A volume of Lipofectamine^{TM} 2000 (equal to the total DNA) volume was added to the DNA. FRET acceptor bleaching experiments were performed using Leica SP5 confocal microscope. LAS AF Suite FRET AB Wizard was used to perform and analyze the FRET acceptor photo bleaching experiment. The donor (EGFP) was excited at 488 nm and the emission signal was detected between 495 and 535 nm. The acceptor (mCherry) was excited at 561 nm and the emission signal was detected between 610 and 665 nm. A large Region of Interest (ROI) was selected and was bleached by the 561 nm laser; typically the acceptor signal reduced ~2-3 fold. Following bleaching of the large regions, co-localized signals within the large ROI were selected for FRET analysis.

Local protein synthesis

5'UTRαCaMKII-dendra2-3'UTRαCaMKII or *dendra2-3'UTRαCaMKII* was transfected into the cultured hippocampal neurons at DIV 5. Nine days after transfection, cells were imaged in buffer containing 145 mM NaCl, 3 mM KCl, 3 mM CaCl2, 10 mM HEPES, 8 mM glucose. We used UV to activate the dendra2 protein in a limited region of dendrites, then BDNF (30ng/ml) was added into cells. Confocal images were acquired with a Leica SP5 confocal microscope (Leica Microsystems Ltd) at 10 minutes intervals for 30 minutes before and after BDNF treatment. For protein inhibition, 100 μM of cycloheximide (Tocris) or 10 μM anisomycin (Alomone lab) was added in media 30 min before and during the experiment. All experiments were performed at 37˚C. The stage was heated to 37°C using an airstream heater.

Calcineurin assay

Calcineurin activity was measured using the calcineurin activity assay kit (Calbiochem). Flag-DSCR1 was immunoprecipitated following addition of Flag antibody coupled agarose beads (Sigma). The agarose beads were then incubated with brain extracts or primary neuronal extracts treated with or without BDNF. After washing the beads several times, calcineurin reaction buffer containing calcineurin and its substrate was added and further incubated for 3 hours at 30˚C. Calcineurin activity was measured according to the manufacturer's protocol.

Western Blotting

Total protein extract was prepared from cell cultures using RIPA lysis buffer. Protein (10–20 μg) was run on SDS polyacrylamide gel and transferred to nitrocellulose membrane. The following primary antibodies were used: DSCR1, phospho-FMRP, FMRP, phospho-cofilin, phospho-serine (Millipore), and β-tubulin (Developmental Studies Hybridoma Bank).

Membranes were stripped using Reblot Plus strong antibody stripping solution (Millipore) and re-probed. ImageJ software was used to measure signal intensity, and the fold change in specific protein level was calculated by comparing to the control.

Statistical Analysis

Statistical values were shown as mean ± SEM. Statistical significances were calculated by using GraphPad Prism 5.0 software (GraphPad Software). Method used for statistical analyses are as listed. Unless indicated otherwise, two-way ANOVA analysis with Bonferroni post test was used if more than two populations were compared with each other. P value of < 0.05 was considered significant.

FIGURE LEGENDS

Figure S1. DSCR1 distribution.

(A) DSCR1 is found in soma, dendrites, and dendritic spines. Phalloidin staining indicates spines. (B) DSCR1 is absent in axonal terminals. Synaptophysin, an axon terminal marker, and DSCR1 do not overlapped. Scale bar, 10μm.

Figure S2. Expression level of DSCR1 in hippocampal neurons.

Neurons containing *DSCR* shRNA reduced DSCR1 level almost 50%, while *DSCR1* overexpression clearly increased DSCR1 level. Sixteen neurons from three independent experiments were measured. Values represent mean ± SEM, and * indicates $P < 0.0001$ as determined by ANOVA analysis. Scale bar, 10μm.

Figure S3. DSCR1 modulates spine morphogenesis.

Hippocampal neurons containing *DSCR1* shRNA show significantly fewer dendritic spines, while neurons having *DSCR1* transgene have larger dendritic spine heads. Inset is shown below. Scale bars are 10 μm (upper) and 5 μm (below).

Figure S4. Expression level of DSCR1 and FMRP in hippocampal neurons transfected with *DSCR1* shRNA and *fmr1* siRNA or *DSCR1* transgene and *fmr1* siRNA.

FMRP is decreased to half by *fmr1* siRNA in neurons containing either *DSCR1* shRNA or transgene, while *DSCR1* transgene increased the level of DSCR1 almost three times. Sixteen neurons from three independent experiments were measured. Scale bar, 10μm. Values shown as mean ± SEM, and tested for statistical significance by ANOVA analysis. * $P < 0.0001$.

Figure S5. DSCR1 levels in *DSCR1*$^{-/-}$ and *DSCR1* transgenic mice and FMRP levels in *fmr1*$^{-/-}$ and *DSCR1* transgenic/*fmr1*$^{-/+}$ mice.

(A) DSCR1 level in the hippocampi of *DSCR1*$^{-/-}$ and *DSCR1* transgenic mice is shown by western blot. n = 3; values represent mean ± SEM. * indicates $P < 0.01$. (B) *DSCR1* transgenic/*fmr1*$^{-/+}$ mice show 50% reduction in the level of FMRP compared to control in the hippocampi. n = 3, values represent mean ± SEM. * indicates $P < 0.002$.

Figure S6. *DSCR1*$^{-/-}$, *DSCR1* transgenic brains show abnormal dendritic spines in the cortical layer V.

(A) Golgi staining of the cortical layer V in wild type, *DSCR1*$^{-/-}$, *DSCR1* transgenic mice. Consistent with hippocampal CA1 pyramidal neurons, *DSCR1*$^{-/-}$ shows reduction in spine density, while *DSCR1* transgenic mouse produced enlarged spine head. Each image is composed from an

average of 30 focused Z-stacks. Scale bar, 10 μm. (B, C) Quantification of dendritic spines on the cortical layer V neurons. Eight neurons from brains of each genotype were used for Golgi staining. Number of spines grouped by distance from the cell body and average spine head area of neurons were analyzed. 50 to 60 spines were used to measure the size. Postnatal 21 days of mice brains were used for the analyses. Values represent mean ± SEM, * indicates $P < 0.0001$ as determined by ANOVA analysis.

Figure S7. DSCR1 overexpression and FMRP reduction restored the level of phospho-cofilin.

(A) HEK cells transfected with *DSCR1* shRNA or *DSCR1* transgene were examined for the level of phospho-cofilin. n = 7; values are shown as mean ± SEM, and tested for statistical significance by ANOVA analysis. * indicates $P < 0.0001$. (B) The level of phospho-cofilin in hippocampal primary neurons transfected with *DSCR1* shRNA or *DSCR1* transgene were altered. FMRP reduction also decreased phospho-cofilin. Reduction of both DSCR1 and FMRP further reduced phospho-cofilin, while neurons having DSCR1 overexpression and FMRP reduction restored the level of phospho-cofilin to normal. n = 7; values represent mean ± SEM. * indicates $P < 0.001$ as determined by ANOVA analysis.

Figure S8. FMRP antibodies.

(A) Immunoprecipitation with phospho-FMRP antibody was followed by blotting with phospho-FMRP and FMRP antibodies. (B) Immunoprecipitation with FMRP antibody was followed by blotting with FMRP and phospho-FMRP antibodies. FMRP and phospho-FMRP antibodies show clear preference toward non-phosphorylated FMRP and phospho-FMRP, respectively. HEK cells were used for immunoprecipitation. (C) HEK cells transfected with either *Flag-His-*

FMRP or *Flag-His-FMRP*$^{(S499\ to\ A)}$ together with *DSCR1* were immunoprecipitated with Flag antibody and the Western blot was detected with antibodies as indicated. Phosphorylation competent Flag-His-FMRP co-immunoprecipitated with DSCR1 but phosphorylation defective Flag-His-FMRP$^{(S499\ to\ A)}$ did not bind to DSCR1. The blot was also stripped and detected with the His antibody to ensure that the same amount of proteins were pulled down. * indicates nonspecific band. Input: HEK cells transfected with *Flag-His-FMRP*.

Figure S9. DSCR1 is required for local protein synthesis.

(A) Dendra-2 construct in hippocampal neurons before and after photo-activation (outlined circle in left panel). Panel below shows pseudo-colored images of the green fluorescent dendra2 proteins in dendritic spines before and after photoconversion. (B) Primary neurons transfected with *DSCR1* shRNA, *DSCR1* transgene, or *fmr1* siRNA. Neurons transfected with both *DSCR1* transgene and *fmr1* siRNA were also used. Scale bar, 1 μm. (C) The change in intensity of fluorescence was analyzed in three different regions: near to soma (in), spine, and away from soma (out) for 30 min with BDNF stimulation. Neurons at DIV 14 were used for the analyses. n = 24 spines in each condition from 3 independent experiments, * $P < 0.03$. Values are shown as mean ± SEM, and tested for statistical significance by ANOVA analysis.

Figure S10. Local protein synthesis occurs only after BDNF treatment.

(A) In the absence of BDNF treatment, no change in dendra-2 signals was found in the primary hippocampal neurons of *DSCR1*$^{-/-}$, *DSCR1* transgenic, and *fmr1*$^{-/-}$. (B) When anisomycin is added, BDNF failed to trigger local protein synthesis in dendritic spines.

Figure S11: BDNF treatment does not change the level of FMRP.

(A) The level of FMRP in hippocampal neurons remains mostly unchanged before and after BDNF treatment. Twelve neurons from three independent cultures were measured. Scale bar, 10 μm. (b) Phospho-FMRP is decreased in the brain of *DSCR1*$^{-/-}$. n = 3; values represent mean ± SEM. * P = 0.05 as determined by Student's t-test.

Figure S12. A model for regulation of local protein synthesis by DSCR1 and FMRP.

(A) In early stages of spine morphogenesis during development, DSCR1 affects the level of phospho-cofilin through calcineurin, which subsequently modulates spine head size. FMRP can also influence cofilin dynamics through PP2AC. (B) At resting dendritic spines, DSCR1 and phospho-FMRP complex inhibit calcineurin activity and repress local protein synthesis. However, upon BDNF stimulation, an endogenous kinase is activated, which phosphorylates DSCR1. Subsequently, phosphorylated DSCR1 allows calcineurin activation, thus cause dephosphorylation of phospho-FMRP originally bound to target mRNAs. This then prompts the release of FMRP, thus allowing protein synthesis to occur. Newly synthesized proteins involved in local actin dynamics will shape spine morphology together with the phosphorylation status of phospho-cofilin. Phosphorylated DSCR1 is subsequently returned to dephosphorylated DSCR1, thus inhibits calcineurin activity. Together, these events will influence spine morphology.

Figure S1. Wang et al.

A

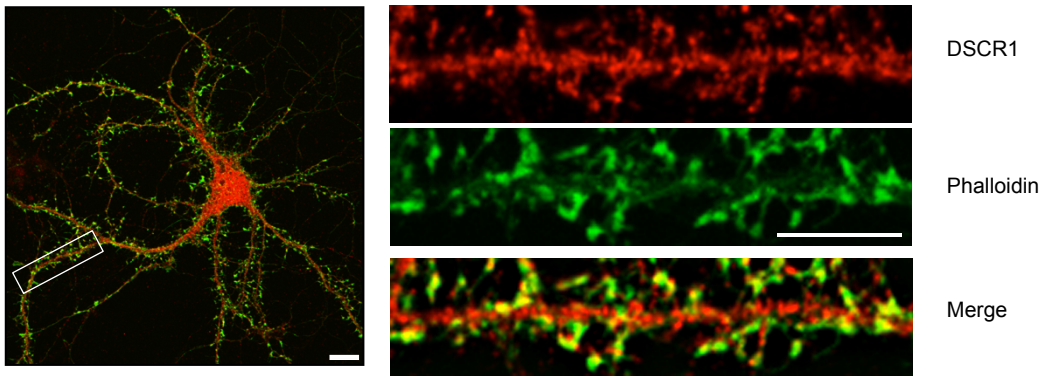

B

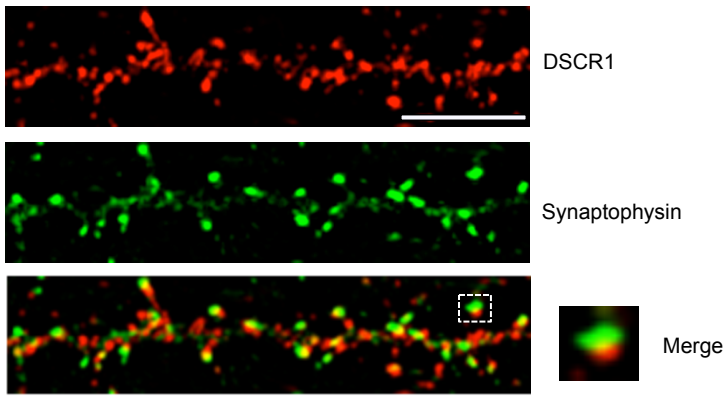

Figure S2. Wang et al.

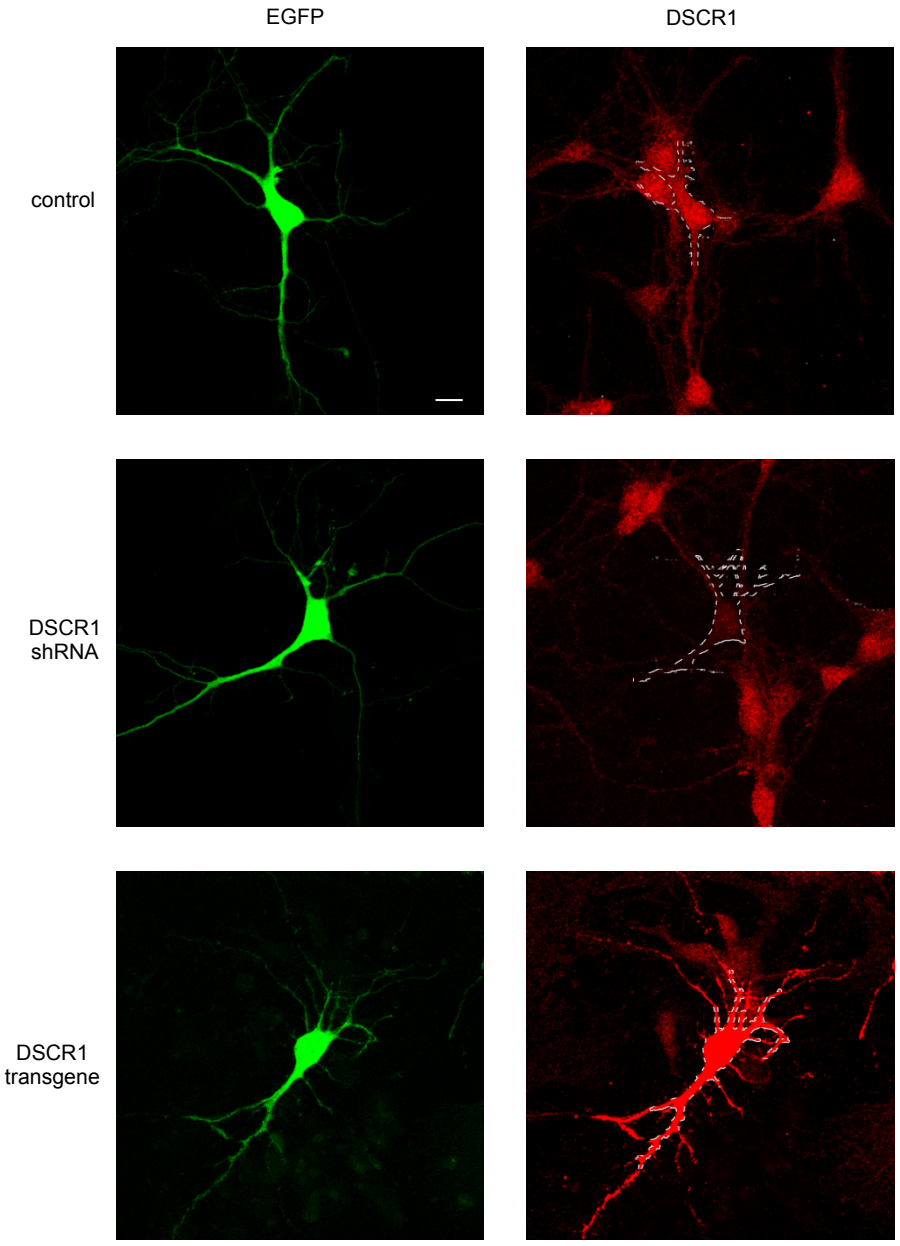

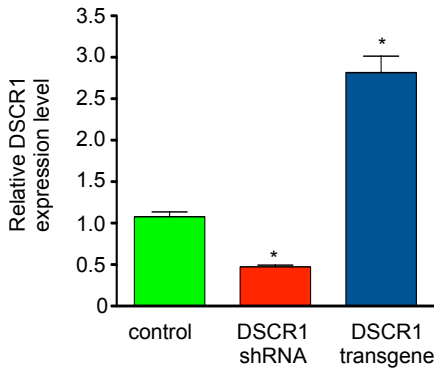

Figure S3. Wang et al.

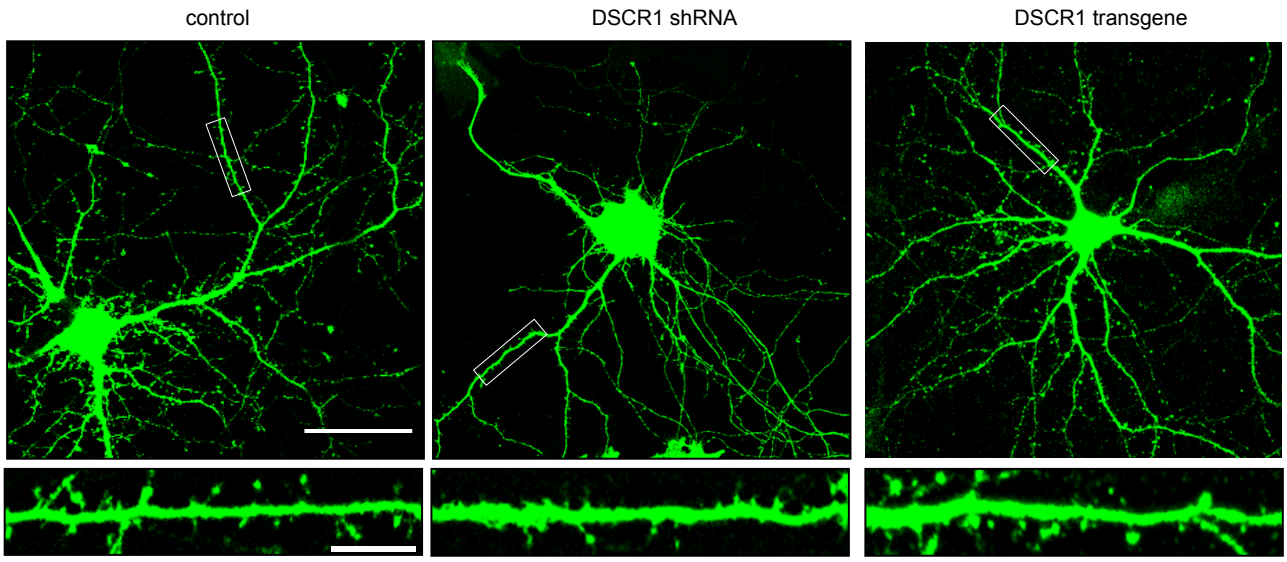

Figure S4. Wang et al.

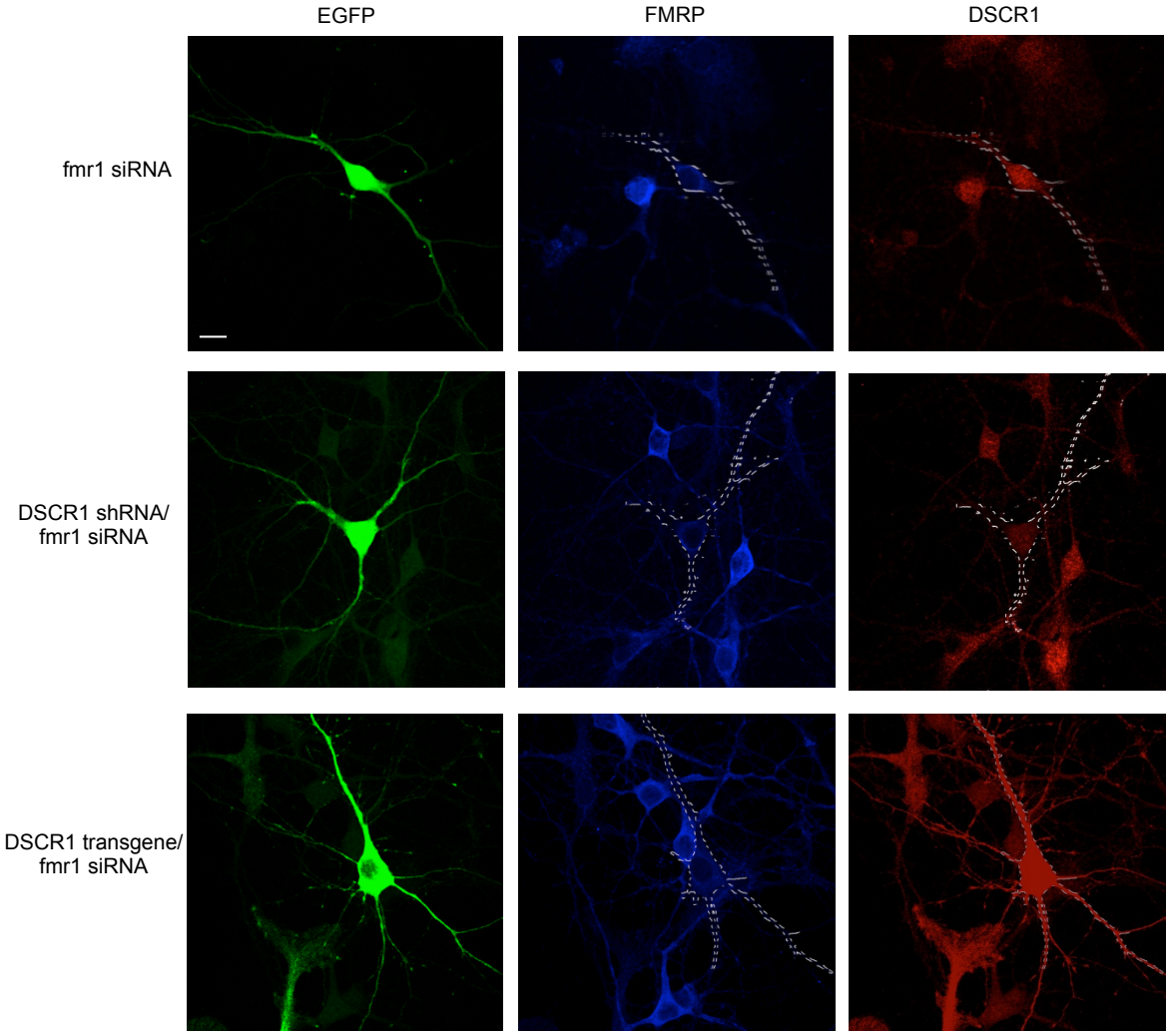

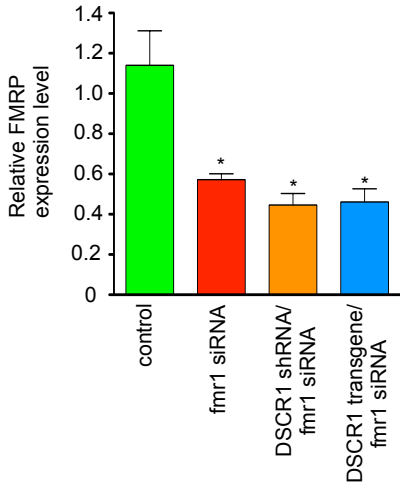

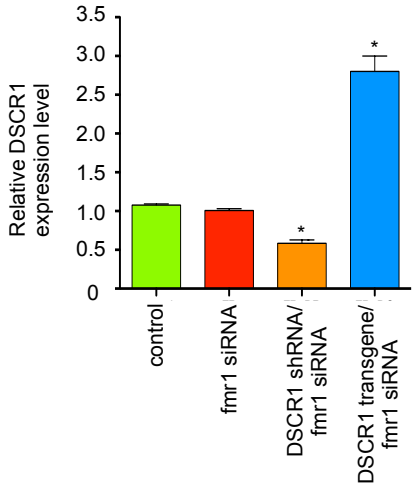

Figure S5. Wang et al.

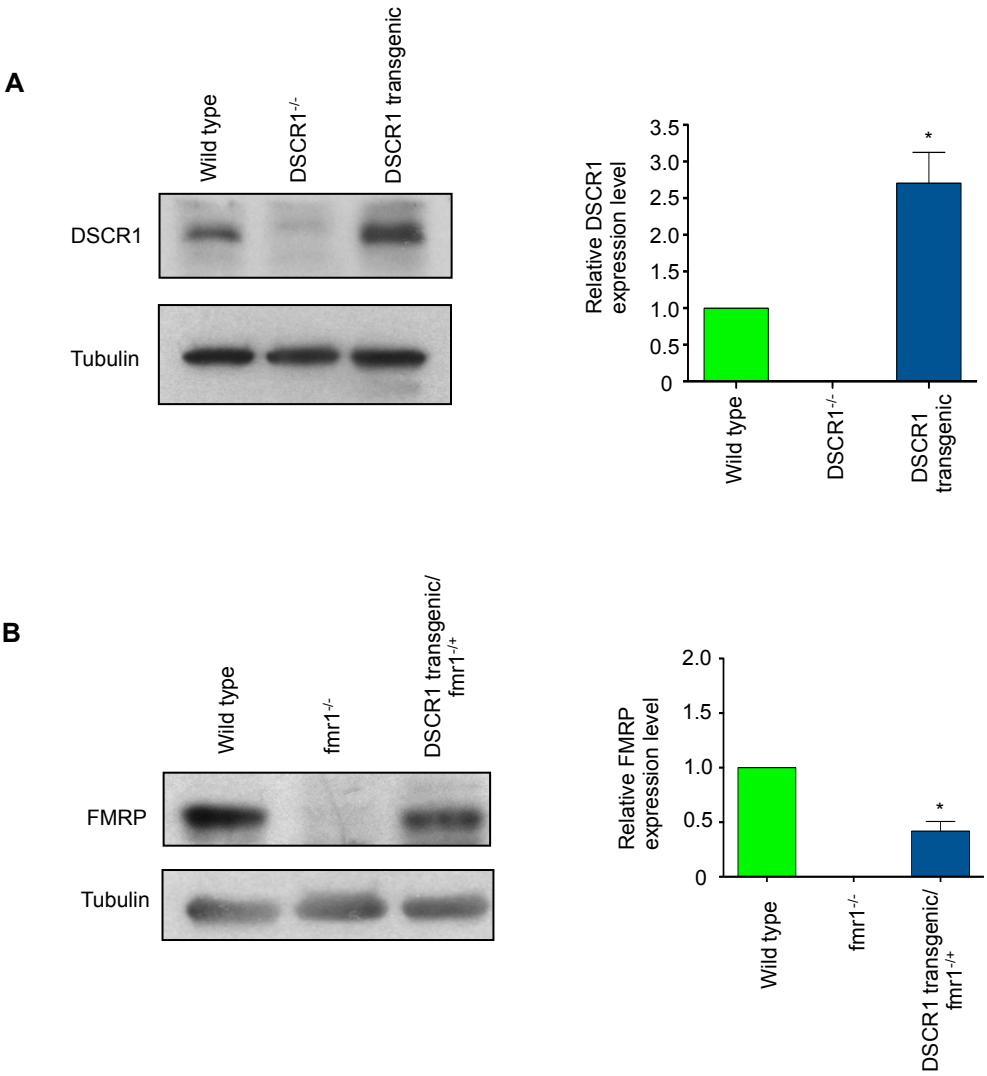

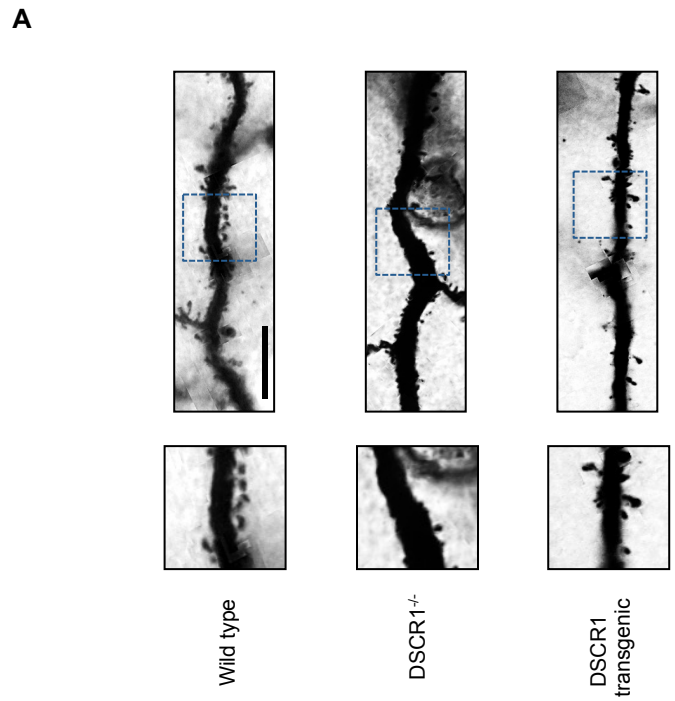
A
Wild type
DSCR1-/-
DSCR1 transgenic

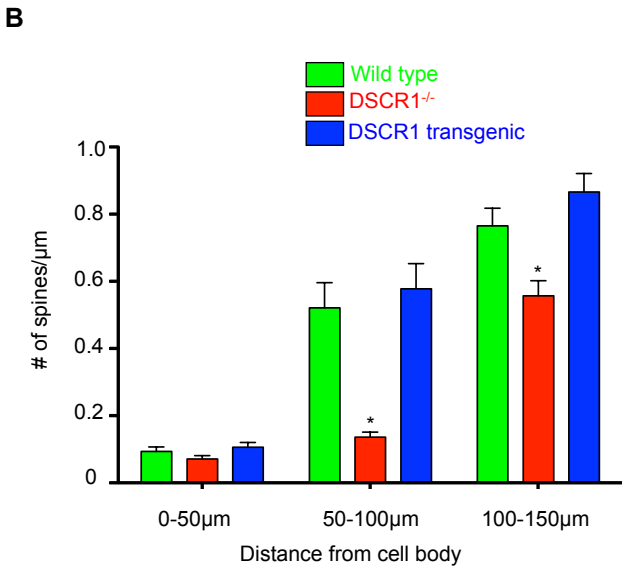
B
Wild type
DSCR1-/-
DSCR1 transgenic
# of spines/µm
1.0
0.8
0.6
0.4
0.2
0
0-50µm
50-100µm
100-150µm
Distance from cell body

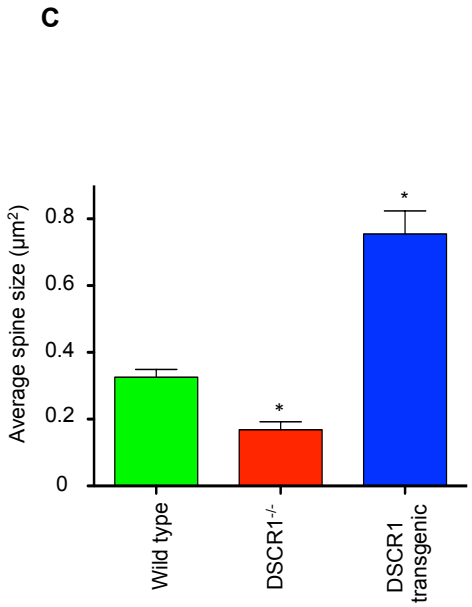
C
Average spine size (µm2)
0.8
0.6
0.4
0.2
0
Wild type
DSCR1-/-
DSCR1 transgenic

Figure S7. Wang et al.

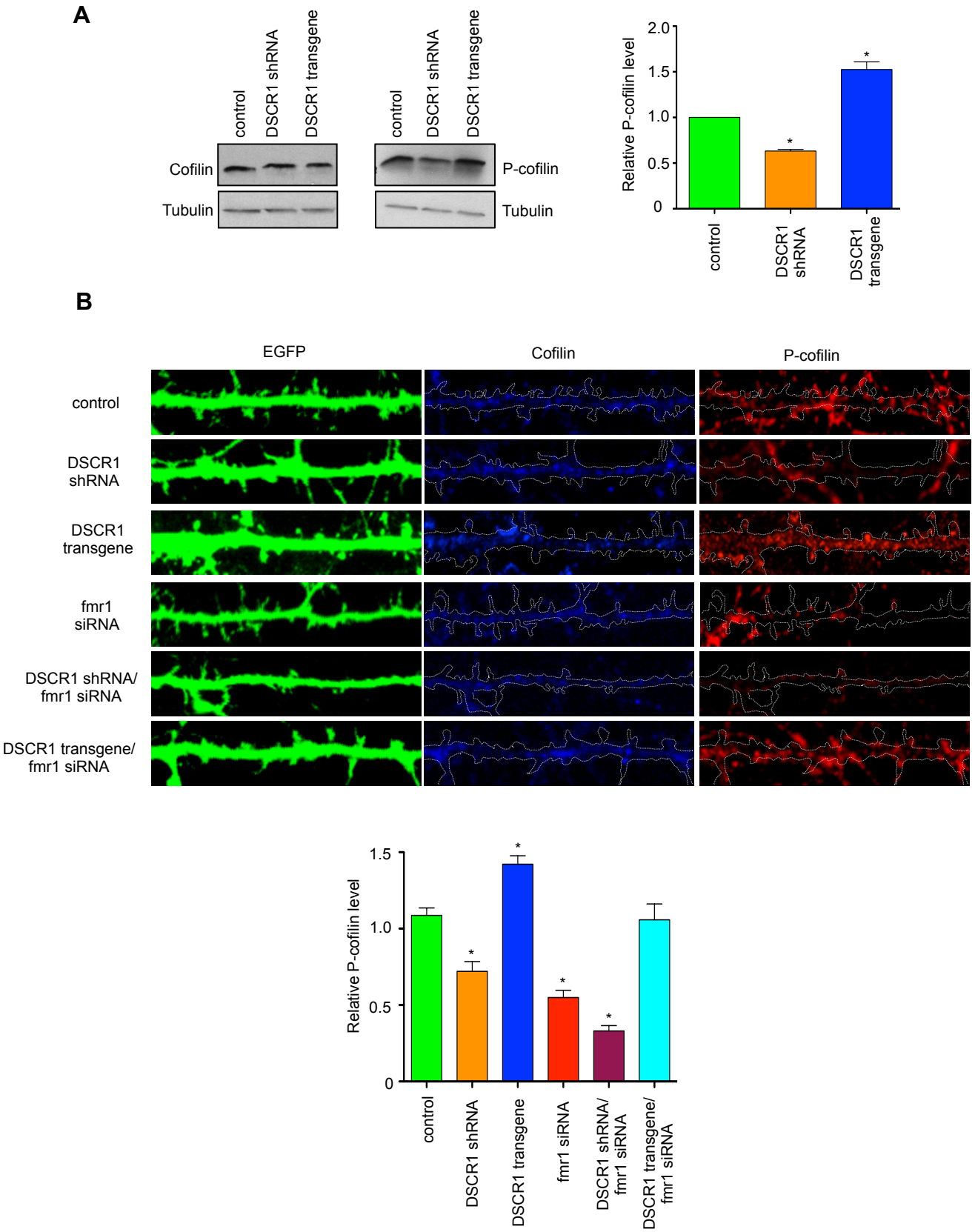

Figure S8. Wang et al.

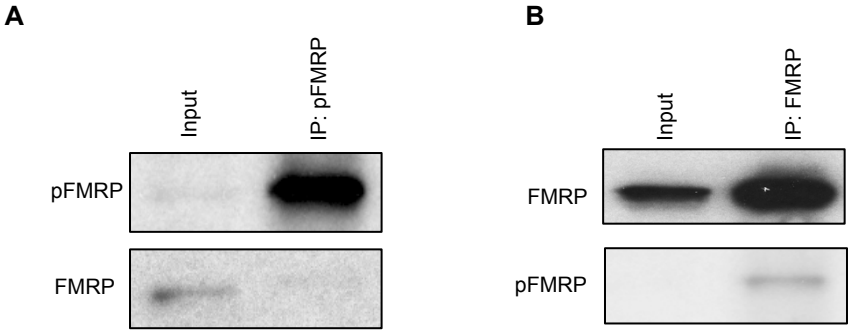

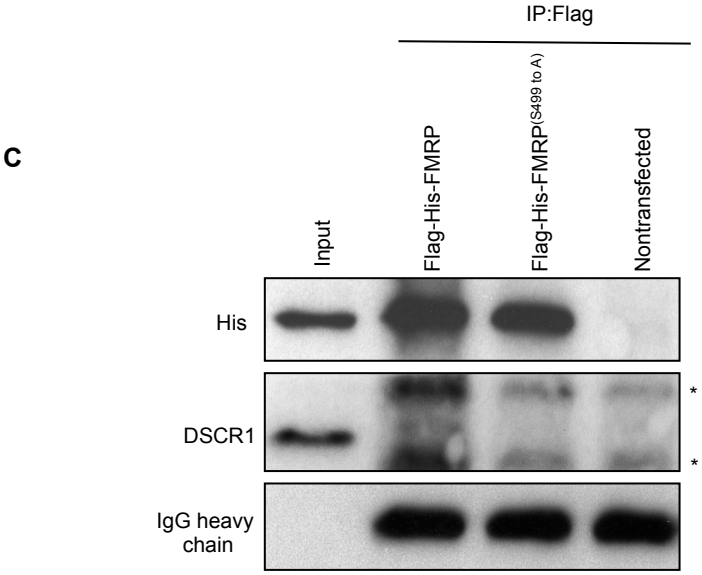

Figure S9. Wang et al.

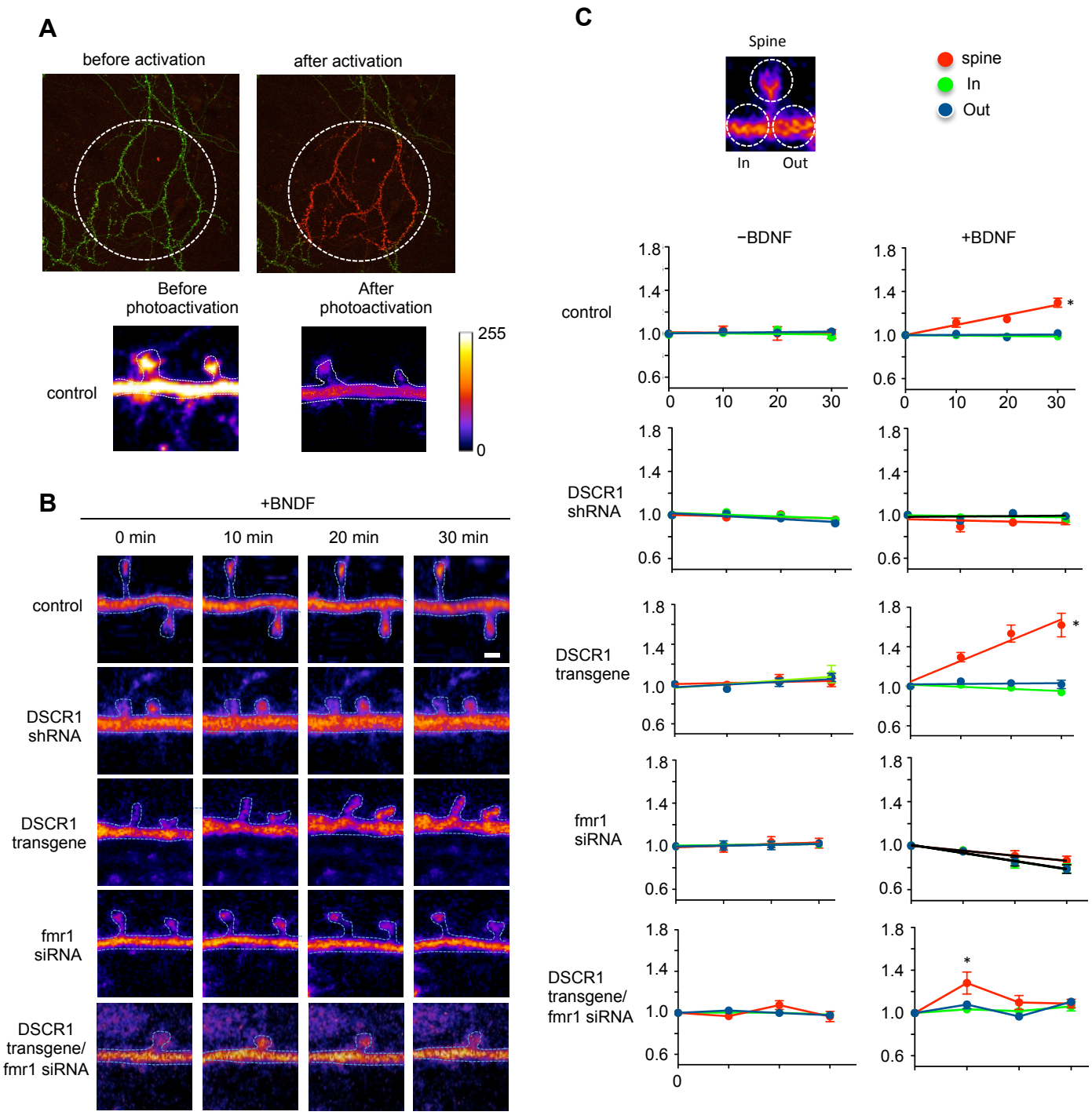

Figure S10. Wang et al.

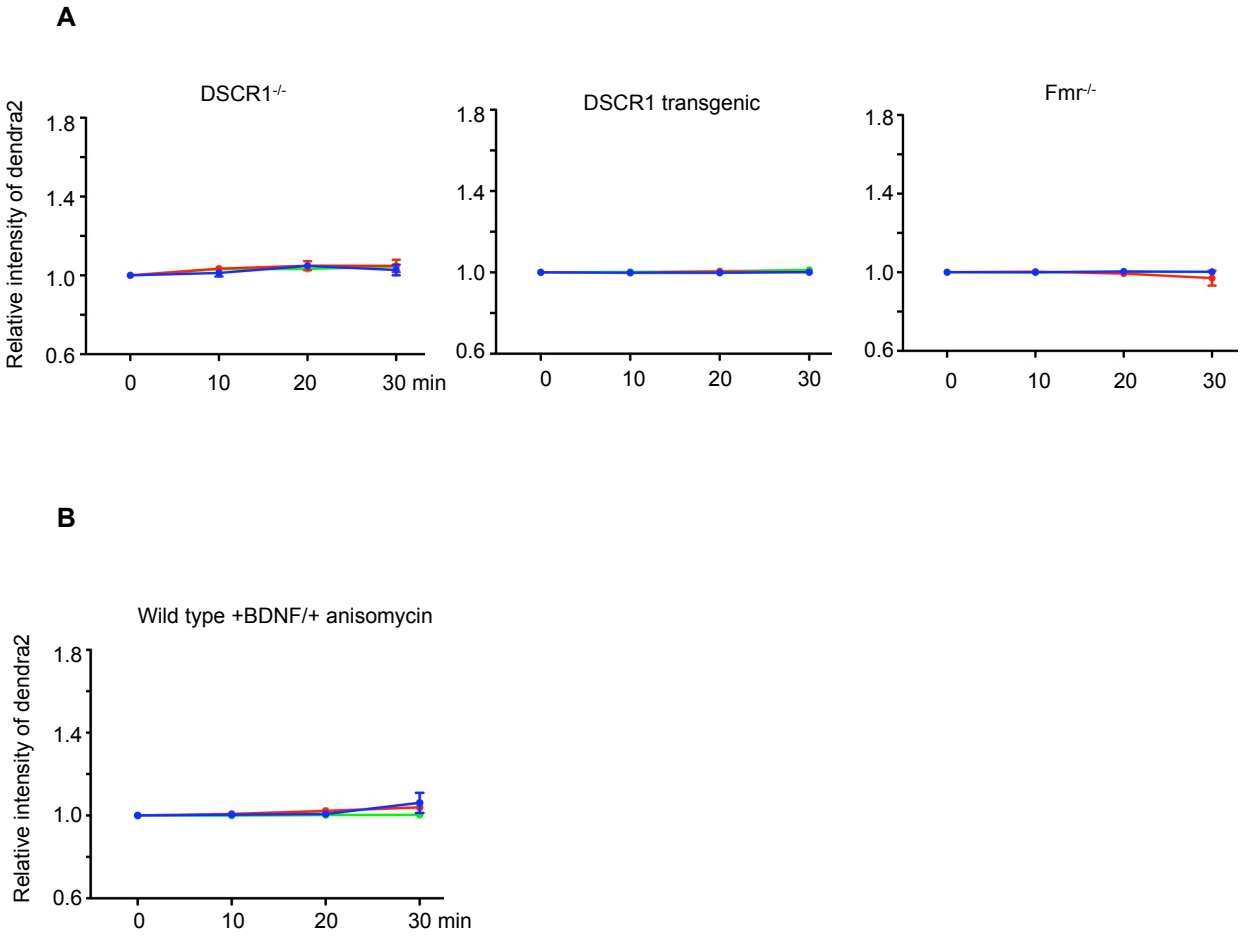

Figure S11. Wang et al.

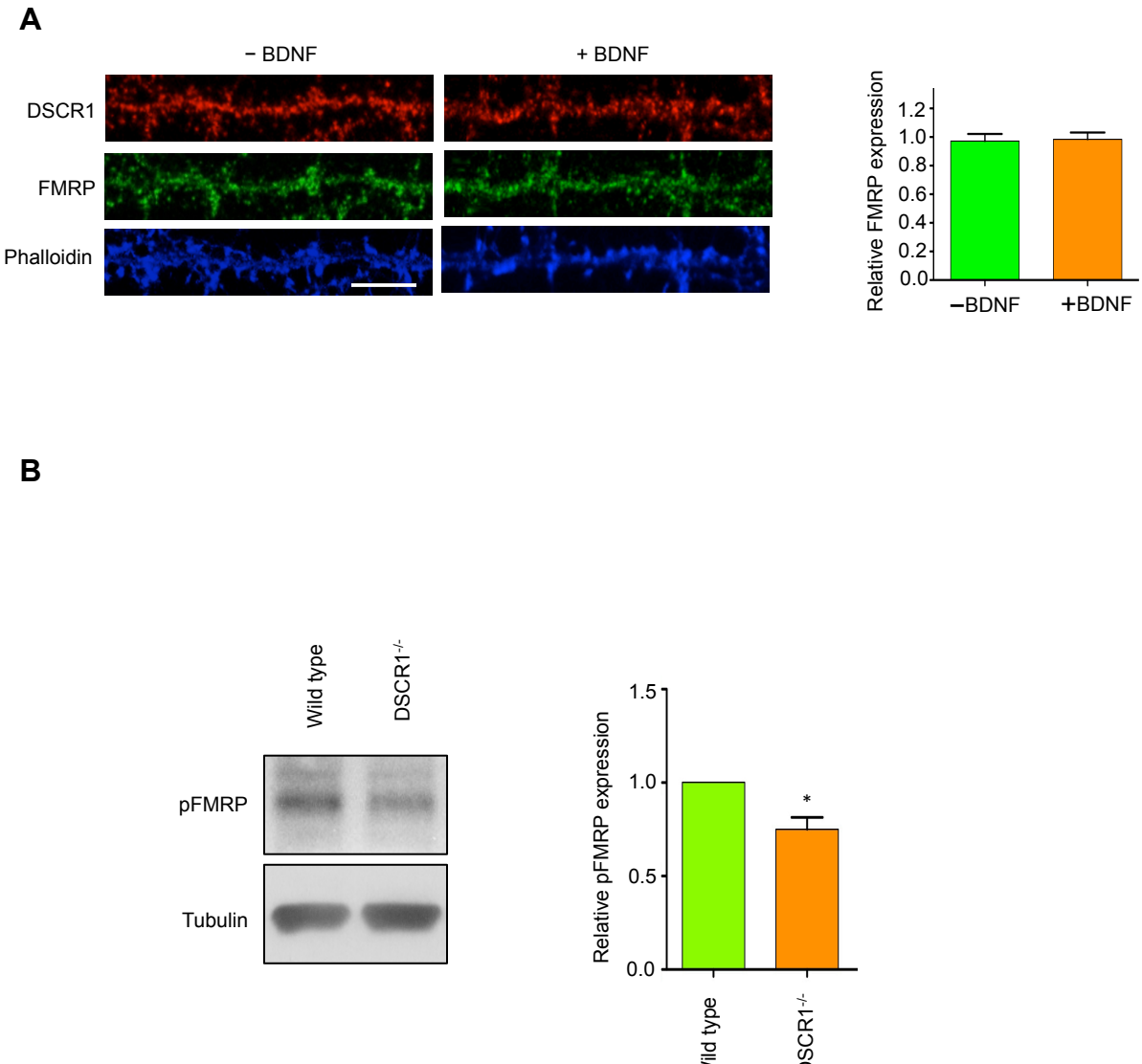

Figure S12. Wang et al.